

UNCLASSIFIED

AD _405 474 _

DEFENSE DOCUMENTATION CENTER

FOR

SCIENTIFIC AND TECHNICAL INFORMATION

CAMERON STATION, ALEXANDRIA, VIRGINIA



UNCLASSIFIED

NOTICE: When government or other drawings, specifications or other data are used for any purpose other than in connection with a definitely related government procurement operation, the U. S. Government thereby incurs no responsibility, nor any obligation whatsoever; and the fact that the Government may have formulated, furnished, or in any way supplied the said drawings, specifications, or other data is not to be regarded by implication or otherwise as in any manner licensing the holder or any other person or corporation, or conveying any rights or permission to manufacture, use or sell any patented invention that may in any way be related thereto.

63-3-5

405474

ASTIA Document No. AD-

THIRD QUARTERLY TECHNICAL NOTE

on a

STUDY OF MULTI-FUNCTION SENSORS
FOR GUIDANCE SUBSYSTEMS

Prepared by
Alan Bloch

GENERAL PRECISION, INC.
Tarrytown, New York

May 1963

Contract No. AF33(657)-9207

Aeronautical Systems Division
Wright-Patterson Air Force Base
Ohio

7107 1112
1300
MAY 1963

405 474

NOTICES

When Government drawings, specifications, or other data are used for any purpose other than in connection with a definitely related Government procurement operation, the United States Government thereby incurs no responsibility nor any obligation whatsoever; and the fact that the Government may have formulated, furnished, or in any way supplied the said drawings, specifications or other data, is not to be regarded by implication or otherwise as in any manner licensing the permission to manufacture, use or sell any patented invention that may in any way be related thereto.

Qualified requesters may obtain copies of this report from the ASTIA Document Center, Arlington Hall Station, Arlington 12, Virginia. ASTIA Services for the Department of Defense contractors are available through the "Field of Interest Register" on the "need-to-know" certified by the cognizant military agency of their project or contract.

ASTIA Document No. AD-

THIRD QUARTERLY TECHNICAL NOTE
on a
STUDY OF MULTI-FUNCTION SENSORS
FOR GUIDANCE SUBSYSTEMS

Prepared by

Alan Bloch

GENERAL PRECISION, INC.
Tarrytown, New York

May 1963

Contract No. AF33(657)-9207

Aeronautical Systems Division
Wright-Patterson Air Force Base
Ohio

FOREWORD

This report was prepared by General Precision, Inc., Tarrytown, New York, on Contract AF33(657)-9207, Project Nr. 4427 with the Aeronautical Systems Division, Wright-Patterson Air Force Base, Ohio. The work was administered under the direction of Mr. C. Coombs of ASD.

The work reported herein covers the period from 1 January, 1963 to 31 March, 1963 and was performed under the direction of A. Bloch, Program Manager for GPI. Principal contributors were L. Goldfischer and A. Miccioli of GPL and W. Davis of Librascope.

This report covers the third quarter of a one year program ending 30 June 1963.

ABSTRACT

The purpose of the program ~~described herein~~ is the ~~ultimate~~ development of multi-function sensors for space-vehicle guidance and navigation. This third quarterly report contains detailed discussions of the work carried out by the contractor during the reporting period. A section is devoted to the theory of overlapping Fresnel zone plates. Plans for the next quarter are discussed briefly.

TABLE OF CONTENTS

	<u>Page</u>
1. INTRODUCTION.	1
2. BACKGROUND.	3
3. WORK DURING THE CURRENT QUARTER	5
3.1 GPL Division Effort.	5
3.2 Librascope Division Effort	6
4. PLANS FOR THE NEXT QUARTER.	7
4.1 GPL Division Fourth Quarter Plans.	7
4.2 Librascope Division Fourth Quarter Plans	7
APPENDIX A - THE NEED FOR STAR FIELD TRACKING ON RENDEZVOUS MISSIONS.	A-1 - A-3
APPENDIX B - IMAGE CORRELATION IN THE LIBRASCOPE STEREO PLOTTER	B-1
APPENDIX C - COMPARISON OF HOLOGRAM AND OVERLAPPED ZONE PLATES FOR A FIELD CONSISTING OF TWO POINTS.	C-1 - C-16
APPENDIX D - SIMULTANEOUS TRACKING OF STAR FIELD AND COOPERATIVE SPACE VEHICLE	D-1 - D-2
APPENDIX E - BEACON POWER REQUIRED ABOARD COOPERATIVE SPACE VEHICLE	E-1 - E-7

LIST OF ILLUSTRATIONS

<u>Figure</u>		<u>Page</u>
C-1	GEOMETRY FOR CALCULATION OF INTERFERENCE FRINGE PATTERN.	C-2
C-2	HOLOGRAM - CENTRAL SECTION	C-7
C-3	HOLOGRAM - SECTION DISPLACED FROM CENTER BY HALF THE THE SEPARATION OF POINT SOURCES.	C-8
C-4	OVERLAPPED ZONE PLATES - ZONE PLATE CENTERS OPAQUE .	C-9
C-5	OVERLAPPED ZONE PLATES - ZONE PLATE CENTERS CLEAR. .	C-10
C-6	OVERLAPPED ZONE PLATES - ENLARGED CENTRAL SECTION. .	C-11
C-7	OVERLAPPED ZONE PLATES - ENLARGED SECTION AROUND ONE ZONE PLATE CENTER.	C-12
C-8	OVERLAPPED ZONE PLATES - ENLARGED SECTION BETWEEN CENTER OF ONE ZONE PLATE AND CENTER OF OVERLAP REGION	C-13
C-9	HOLOGRAM - SECTION EQUIVALENT TO OVERLAPPED ZONE PLATE (FIG.C-8).	C-14
E-1	CROSS SECTIONAL SKETCH OF BEACON	E-7

1. INTRODUCTION

The broad objective of the work reported here is, ultimately, the development of one or more multi-function sensors for space-vehicle guidance and navigation. The more limited objective of the present contract is the development of concepts and preliminary designs in terms of their suitability for possible further development work.

Although the use of multi-function sensors offers some possibility of reduction in overall system size, weight, and power consumption, the primary reason for developing these sensors is the promise of improvement in overall system reliability. A single multi-function sensor may or may not be preferable to the equivalent set of special-purpose sensors. A redundant set of multi-function sensors, however, is almost certain to offer higher reliability than the equivalent non-redundant set of special-purpose sensors.

Another way of improving system reliability is through reduction in the computing load. For example, a multi-function sensor might stabilize itself (function 1) by locking on to the celestial sphere (star-field tracking) and simultaneously track a target for rendezvous (function 2) directly in celestial coordinates. The alternative straightforward approach involves star-field or multiple-star tracking to determine vehicle orientation, target tracking in a vehicle coordinate system, and computation to convert the observed (body-axis) target coordinates to absolute (celestial) target coordinates.

A brief discussion of the desirability of carrying out the rendezvous calculations in a coordinate system fixed to the celestial sphere is included in this report as Appendix "A".

For the present, at least, the program is limited to the field of optical sensors --- but with no restriction to the visible portion of the optical spectrum. A further limitation on the initial work is that the sensor functions considered should be appropriate to operation

in cis-lunar space.

Two sorts of multi-function sensors come immediately to mind. One is a GPL correlator with presently-available terrain-matching capability and with, at least, added starfield tracking capability. The other is a combination of TV pickup and edge-sensing capabilities, making use of Librascope techniques. Work during this quarter has been oriented toward the first of these; however a brief discussion of the correlation techniques used in the Librascope Stereoplotter has been included in this report as Appendix "B". This discussion supplements Appendix "B" of the First Quarterly Report, which describes another embodiment of the Librascope correlation technique.

2. BACKGROUND

By the end of the last quarter (October, November, December 1962) the immediate aims of the program were fairly definite, and the following decisions had been reached.

- 1) The program is oriented around the GPL correlator, and the major objective is that of moving the starfield tracking capability toward a level approximating that of the current terrain-matching capability. This route leads to the possibility of a Multi-Function Sensor capable of either starfield tracking or terrain matching.
- 2) A secondary objective of the program is that of developing dual-mode capability for the starfield tracker. This involves simultaneous tracking of the star field and tracking of a cooperative target (which need not be on the optical axis of the correlator). The usefulness of such an instrument is briefly discussed in Appendix "A".
- 3) It was decided that work on the starfield tracker would be directed toward a lensless GPL correlator using a reference composed of overlapping Fresnel zone plates. An instrument of this sort was tested in the laboratory with excellent results. Fabrication of suitable Fresnel zone plate references appears to be well within the present state-of-the-art.
- 4) Following a rough study of starfield statistics, it was decided that the starfield tracker would make use of post-correlation image intensification. Image intensifiers having the required gain and resolution appear to be within the present state-of-the-art, although none are currently available as shelf items. It is noted that terrain-matching may require a different detector than starfield tracking, so that a sensor having both of these capabilities might need two detectors with provision for bringing one or the other into operation.

- 5) Although decisions were reached regarding the requirement for an image intensifier and regarding its optimum position in a functioning starfield tracker, no further work in this direction will be attempted. The present program will be limited to laboratory equipment where such an intensifier is not required, and current funding does not permit anything more than brief investigation of intensifier characteristics and availabilities.

The program, thus limited and brought into sharper focus, appears to be completely feasible and has already yielded useful results.

3. WORK DURING THE CURRENT QUARTER

Work during the current quarter was primarily aimed at moving toward the starfield tracking capability of the GPL correlator. A smaller effort was devoted to the problem of dual-mode operation of the correlator (simultaneous starfield and off-axis target tracking). A minimum effort was devoted to describing an embodiment, different from that described in Appendix "B" of the First Quarterly Report, of the Librascope correlation technique.

3.1 GPL Division Effort

A major effort at GPL Division was devoted to an analysis of the hologram produced by a pair of coherent point sources and a collimated beam. This study was directed at finding the equivalences and differences between such a hologram and a pair of overlapped zone plates. It was shown that the equivalences predominate while the differences appear only in the fine detail. Hence, either the interferometrically derived hologram or the equivalent set of overlapped zone plated may serve equally well for the starfield reference. Since it is known, on theoretical grounds, that the hologram reference will produce no spurious images, it may be inferred that the images produced by the overlapped zone plates will be similarly free of spurious responses. The study is included in this report as Appendix "C".

A bench model of the dual-mode correlator was set up and tested. Separation of the two signals was achieved by modulating the simulated target at 75 cps --- the starfield pattern being modulated by the azimuth jitter frequency of 25 cps. Separation of the output signals was by synchronous detection. A discussion of the advantages offered by dual-mode operation of this sort is included in this report as Appendix "A".

This test was ambitious in that an attempt was made to use the same detector for both sets of signals. A set of overlapping zone

plates served as a reference for the star field. Simultaneously, a single zone Fresnel plate served to focus the image of the simulated target. Advantage was taken of the narrow band characteristics of the Fresnel zone plates in order to minimize modification of one image by the reference associated with the other. A blue filter was placed in front of the simulated star field, and a red filter was used for the simulated target. The two references were then scaled to focus light of the appropriate wavelength on the detector plane.

The results were encouraging and will be followed up in detail using better optical filters. A description of this experiment is included in this report as Appendix "D".

With a view toward the possibility of successful dual-mode operation, calculations were made to determine the power that might be required for a modulated beacon on the cooperating target. These are included in this report as Appendix "E".

3.2 Librascope Division Effort

Work at Librascope proceeded at a relatively low level by virtue of the fact that funds have been taken away from this Division and given to GPL.

A study is going forward covering energy levels and spectral characteristics of stars. The earlier study in this area, carried out at GPL and reported as Appendix "B" of the Second Quarterly Report, aimed only at a determination of how much (if any) image intensification would be required for starfield tracking. The current study at Librascope is designed to provide information for optimum choice of the two wavelengths involved in dual-mode operation with a single detector. No significant results are yet available, but the material will be included in the Final Report.

A brief discussion of the Librascope image correlation technique as embodied in the Librascope Stereoplotter is included in this report as Appendix "B".

4. PLANS FOR THE NEXT QUARTER

Plans for the next quarter are aimed at further enhancement of the desired starfield tracking capability of the GPL correlator and at further work toward perfection of the dual-mode concept (simultaneous tracking of a starfield and an off-axis target).

4.1 GPL Division Fourth Quarter Plans

GPL will proceed further with work on the laboratory version of the starfield tracker. In particular, one avenue which will be explored is that of improving signal-to-noise ratio through the use of higher resolution film for the Fresnel plate starfield reference.

Further work will be carried out on the dual-mode concept. In particular, tests are contemplated using better filters for spectral separation of the simulated star field from the simulated target. In addition, the use of high resolution film material will be explored in this connection, as well as for the simple starfield tracker.

If it appears to be justified, on the basis of the Librascope study described below, further work will be carried out on the calculation of the power level required for a beacon (to be mounted on a cooperating vehicle) for dual-mode operation.

4.2 Librascope Division Fourth Quarter Plans

Studies of star spectra and energy levels will be carried out to provide inputs to GPL Division for furthering development of the dual-mode concept.

A comprehensive report will be prepared covering all aspects of the Librascope image correlation technique.

APPENDIX A

THE NEED FOR STAR FIELD TRACKING ON RENDEZVOUS MISSIONS

To carry out a rendezvous mission when moving under the influence of a central force field requires sensing and guidance capabilities of substantial complexity. Under conditions of limited thrust and because of the need to minimize fuel consumption, the required maneuvers resemble those of the conventional pursuit course (on or near the surface of the earth) only during the terminal or docking phase of the mission. In order to make such a terminal maneuver at all possible in a practical sense, it is necessary that the initial phase of the mission be devoted to bringing the two orbital planes approximately into alignment and that the midcourse phase be devoted to making the orbits approximately tangential. The rotation of the orbital plane is best accomplished at one of the two points where the trajectory of the rendezvous vehicle crosses the orbital plane of the vehicle being tracked. The initiation of the mission must be timed in such a way that the two vehicles occupy the tangential portions of their orbits simultaneously.

There are two basic reasons why the constraints described in the preceding paragraph are applicable. In order to appreciate the situation, suppose for the moment that it would be possible to achieve rendezvous by direct application of conventional pursuit techniques. This implies that it is possible to achieve velocities considerably in excess of ordinary orbital velocities in a relatively instantaneous manner. The high velocities are required in order to avoid the trajectory bending influence of the central force field. However, this also implies virtually unlimited thrust capabilities from the vehicle rocket engine, certainly well in excess of what is currently available. Even if the large thrust requirements could be met, there would still remain the obstacle of payload capacity. Thrust (which may be equated

to the rate of change of momentum) is achieved in a rocket engine by the expulsion of mass. When operating outside the atmosphere, all of the mass to be expelled must be carried along during all preceding phases of the flight. The more thrust required to accomplish a mission, the smaller the payload capacity of the vehicle. All of the foregoing leads inescapably to the conclusion that minimum thrust, minimum fuel constraints must be placed on the rendezvous mission in a central force field.

The simplest frame of reference for describing the various forces and motions occurring during the rendezvous mission is a non-rotating coordinate system with its origin at the center of the dominant force field. Such a coordinate system is essentially an inertial frame since it is invariant with respect to the fixed stars in the celestial sphere. The simplicity achieved through the use of this frame is primarily computational. To begin with, the equations of motion have their simplest form when written for an inertial frame with the force field centered at the origin. Secondly, non-uniformities in the central field and the gravitational effects of distant bodies may be treated as perturbations, with all the avoidance of computational complexity that this implies.

The orbital parameters of the rendezvous vehicle may be computed from observations of the time variation of the angle between the line of sight to the center of attraction and the direction of a given star field. Using the starfield tracker to establish a point of reference on the celestial sphere, the required observations may be processed either by an on-board computer or telemetered back to a computer station on earth.

Tracking the vehicle being pursued against a starfield background now yields the data necessary to compute its orbital parameters. The computation is essentially the same as that required to determine the orbit of a planet (in the solar system) from earthbound observations.

With the knowledge of the orbital parameters of the two vehicles relative to the inertial frame defined by the star field being tracked, it is a relatively straightforward matter to program the necessary thrusts (relative to the same inertial frame) in order to accomplish the rendezvous mission.

In conclusion, a space vehicle equipped with a multi-function sensor capable of locking on to a star field and simultaneously sensing the direction of a cooperative vehicle, needs only the means of sensing the direction of the center of attraction (sun or planet sensor) to compute the orbital parameters of both vehicles and the thrust program required to accomplish rendezvous. With such sensors, the rendezvous mission becomes a self-contained capability, not dependent on the location of earth stations or weather conditions.

APPENDIX C

COMPARISON OF HOLOGRAM AND OVERLAPPED ZONE PLATES FOR A FIELD CONSISTING OF TWO POINTS

The following discussion is concerned with the calculation of the interference pattern, or hologram, produced by two coherent point sources and a collimated beam. It is shown that the resultant interference pattern differs from the corresponding overlapped zone plate pair only in fine detail. Hence, the reconstruction, or focussing, properties of the overlapped zone plate pair and of the actual hologram of a pair of coherent point sources may be expected to be the same except for the small energy diverted to higher order focal points.

For the calculation, the configuration or geometry depicted by Figure C-1 was employed, where S_1 and S_2 , separated by a distance, d , are point sources in the S plane (defined by S_1 , S_2 , and S_0) parallel to the X-Y plane (i.e., the screen or photographic plate). The X axis of the X-Y plane is chosen so that it is parallel to the line defined by the two point sources S_1 and S_2 . The point defined by $x = y = 0$ (or $P_{(0,0)}$) and the midpoint of the distance, d , are such that the line of length, a , defined by these two points is normal to both planes. S_0 is a point in the plane wave front in the S plane which contributes to the intensity at $P_{(x,y)}$ in the X-Y plane. s_1 , s_2 , and s_0 are defined as the distances from points S_1 , S_2 , and S_0 , respectively, to $P_{(x,y)}$.

It is assumed that the light from S_1 , S_2 , and S_0 is derived from a common collimated source which in turn is derived from a monochromatic point source. Hence, all light in the S plane is monochromatic (of wavelength λ) and coherent (of phase angle θ). At $P_{(x,y)}$, the contributions from S_1 , S_2 , and S_0 in terms of amplitude and phase may be expressed - when θ , the reference phase angle, is assumed to be zero, as

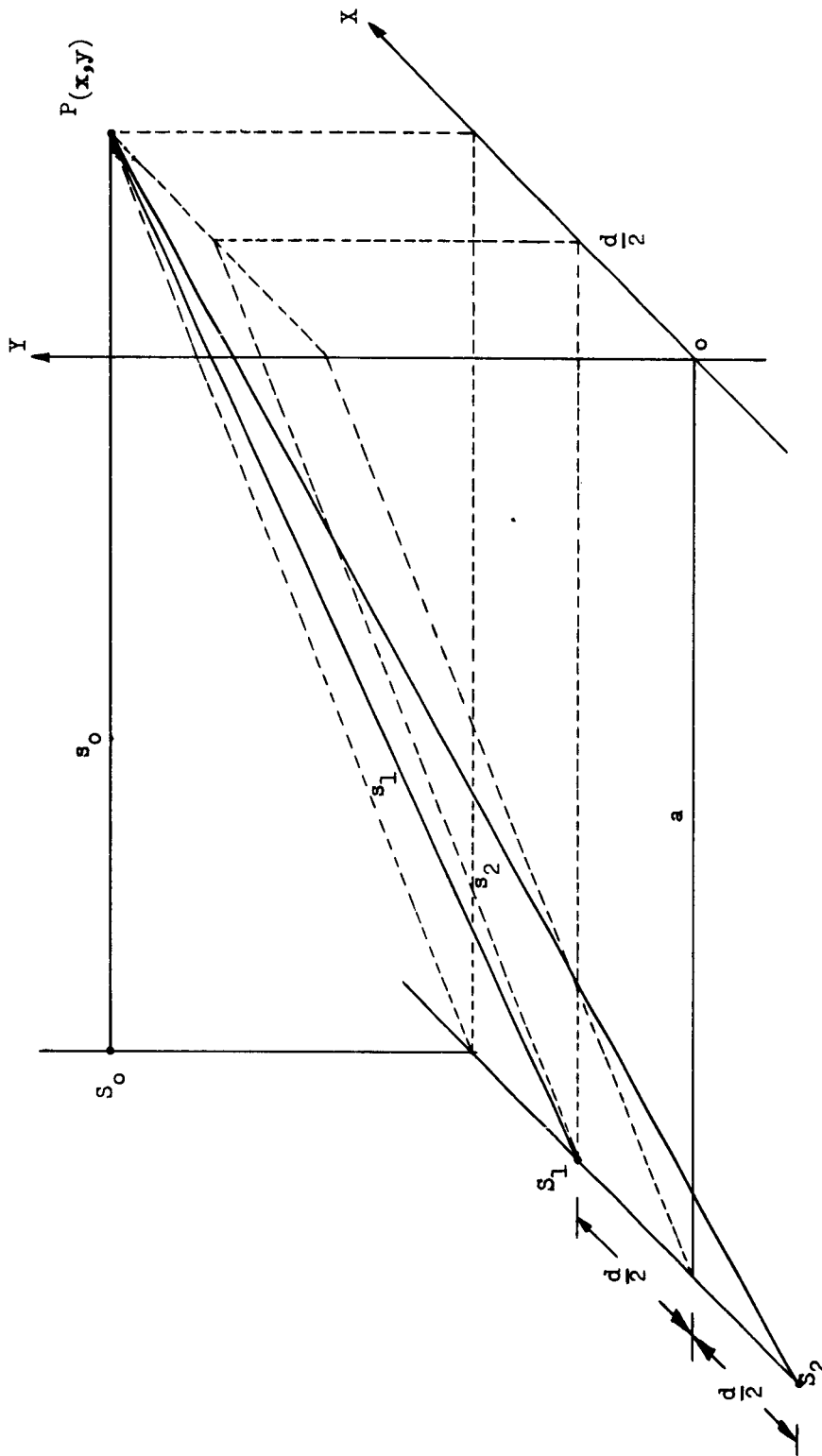


FIGURE C-1 - GEOMETRY FOR CALCULATION OF INTERFERENCE FRINGE PATTERN

$$A_1 \left[\cos \left(-\frac{2\pi}{\lambda} s_1 \right) + j \sin \left(-\frac{2\pi}{\lambda} s_1 \right) \right] \quad (C.1a)$$

$$A_2 \left[\cos \left(-\frac{2\pi}{\lambda} s_2 \right) + j \sin \left(-\frac{2\pi}{\lambda} s_2 \right) \right] \quad (C.1b)$$

$$A_3 \left[\cos \left(-\frac{2\pi}{\lambda} s_0 \right) + j \sin \left(-\frac{2\pi}{\lambda} s_0 \right) \right] \quad (C.1c)$$

where A_1 , A_2 and A_0 are the amplitudes at $P(x,y)$ of the light energy emanating from S_1 , S_2 , and S_0 respectively.

If d is small compared to a , we may let $A_1 = A_2 = A$. Noting, also, that $s_0 = a$, we may rewrite (C.1) as

$$A \left[\cos \left(-\frac{2\pi}{\lambda} s_1 \right) + j \sin \left(-\frac{2\pi}{\lambda} s_1 \right) \right] \quad (C.2a)$$

$$A \left[\cos \left(-\frac{2\pi}{\lambda} s_2 \right) + j \sin \left(-\frac{2\pi}{\lambda} s_2 \right) \right] \quad (C.2b)$$

$$A_0 \left[\cos \left(-\frac{2\pi}{\lambda} a \right) + j \sin \left(-\frac{2\pi}{\lambda} a \right) \right] \quad (C.2c)$$

The intensity I at $P(x,y)$ is proportional to the magnitude of the square of the vector summation of (C.2). Hence,

$$I = A_0^2 + 2A^2 + 2AA_0 \left[\frac{A}{A_0} \cos \frac{2\pi}{\lambda} (s_2 - s_1) + \cos \frac{2\pi}{\lambda} (a - s_2) + \cos \frac{2\pi}{\lambda} (a - s_1) \right] \quad (C.3)$$

Assuming that the distance, a , is an integral number of wavelengths, trigonometric manipulation of (C.3) reduces it to the form

$$I = A_0^2 + 4AA_0 \left\{ \cos \frac{\pi}{\lambda} (s_2 - s_1) \left[\frac{A}{A_0} \cos \frac{\pi}{\lambda} (s_2 - s_1) + \cos \frac{\pi}{\lambda} (s_2 + s_1) \right] \right\} \quad (C.4)$$

To simplify (C.4), we will let A_0 equal $2A$. As a result,

$$I = 4A^2 + 4A^2 \left[\cos \frac{\pi}{\lambda} (s_2 - s_1) \right] \left[\cos \frac{\pi}{\lambda} (s_2 - s_1) + 2 \cos \frac{\pi}{\lambda} (s_2 + s_1) \right] \quad (C.5)$$

From the geometry of Figure C-1, it is evident that

$$s_1 = \sqrt{a^2 + y^2 + \left(x - \frac{d}{2}\right)^2} \quad (C.6a)$$

$$s_2 = \sqrt{a^2 + y^2 + \left(x + \frac{d}{2}\right)^2} \quad (C.6b)$$

Therefore,

$$\begin{aligned} (s_2 - s_1) &= \sqrt{a^2 + y^2 + \left(x + \frac{d}{2}\right)^2} - \sqrt{a^2 + y^2 + \left(x - \frac{d}{2}\right)^2} \\ &= \sqrt{a^2 + \frac{d^2}{4}} \left[\sqrt{1 + \frac{y^2 + x^2 + x d}{a^2 + \frac{d^2}{4}}} - \sqrt{1 + \frac{y^2 + x^2 - x d}{a^2 + \frac{d^2}{4}}} \right] \\ &= \sqrt{a^2 + \frac{d^2}{4}} \left[1 + \frac{1}{2} \frac{y^2 + x^2 + x d}{a^2 + \frac{d^2}{4}} - 1 - \frac{1}{2} \frac{y^2 + x^2 - x d}{a^2 + \frac{d^2}{4}} \right] \\ &= \frac{x d}{\sqrt{a^2 + \frac{d^2}{4}}} \end{aligned}$$

Since $\frac{d^2}{4} \ll a^2$,

$$(s_2 - s_1) \approx \frac{xd}{a} \quad (C.7)$$

In a similar manner

$$(s_2 + s_1) \approx 2a + \frac{y^2 + x^2}{a} \quad (C.8)$$

Substitution of (C.7) and (C.8) into (C.5) yields

$$I = 4A^2 + 4A^2 \left[\cos \frac{\pi}{\lambda} \frac{xd}{a} \right] \left[\cos \frac{\pi}{\lambda} \left(\frac{xd}{a} \right) + 2 \cos \frac{\pi}{\lambda} \left(2a + \frac{y^2 + x^2}{a} \right) \right] \quad (C.9)$$

The term $4A^2$ may be considered to be a bias level of intensity. When the intensity I exceeds $4A^2$, a bright point or constructive interference exists at $P_{(x,y)}$. When I is less than $4A^2$, a dark (or less bright) point or destructive interference exists at $P_{(x,y)}$. The calculation, therefore, reduces to finding the loci of

$$\left[\cos \frac{\pi}{\lambda} \frac{xd}{a} \right] \left[\cos \frac{\pi}{\lambda} \left(\frac{xd}{a} \right) + 2 \cos \frac{\pi}{\lambda} \left(2a + \frac{y^2 + x^2}{a} \right) \right] = 0 \quad (C.10)$$

For the purpose of the calculation, we assumed that

$$d = 0.25 \text{ inches}$$

$$a = 8 \text{ inches}$$

$$\lambda = 0.5 \text{ micron} = 1.97 \times 10^{-5} \text{ inches}$$

Therefore, letting

$$x^2 + y^2 = \rho^2 \quad (C.11a)$$

$$x = \rho \cos \theta, \quad (C.11b)$$

(C.10) may be expressed as

$$\left[\cos (1.5875 \times 10^3 \rho \cos \theta) \pi \right] \left[\cos (1.5875 \times 10^3 \rho \cos \theta) \pi + 2 \cos (6.35 \times 10^3 \rho^2) \pi \right] = 0 \quad (C.12)$$

The solution of (C.12) is not difficult, but it is tedious and time consuming. Hence only two areas were examined in detail, i.e., the area in the vicinity of $x = y = 0$ and the area in the vicinity of $x = 0.125$ inch, $y = 0$. The results, using straight lines to approximate segments of circles, are illustrated by Figures C-2 and C-3. The shaded areas represent regions in which the intensity falls below the bias level of $4A^2$ (due to destructive interference) and the unshaded areas represent regions in which the intensity is above the bias level (due to constructive interference).

Note that Figure C-2 represents the 1st quadrant only. The 2nd quadrant is a mirror image of the 1st, and the 3rd and 4th quadrants are mirror images of the 2nd and 1st quadrants, respectively. Figure C-3, on the other hand, represents the interference pattern for $Y \geq 0$ about the axis $x = 0.125$ inch. For $Y \leq 0$, the pattern is a mirror image of the former.

For purposes of comparison, Figures C-4 through C-8, illustrating overlapped Fresnel zone plates, are included. Figure C-4, represents an overlapped zone plate pair whose central zones are opaque, and Figure C-5 represents an overlapped zone plate pair whose central zones are transparent. Note the presence of what were termed "pseudo" or secondary zone plates in previous reports.

Figures C-6, C-7, and C-8 are enlargements of the indicated areas of Figure C-4. Figure C-6 is an enlargement of the 1st quadrant of the area in the vicinity of $x = y = 0$ and corresponds to the pattern of Figure C-2. Figure C-7, on the other hand, is an enlargement of the region of the overlapped zone plate pair, equivalent - in terms of position - to the pattern of Figure C-3.

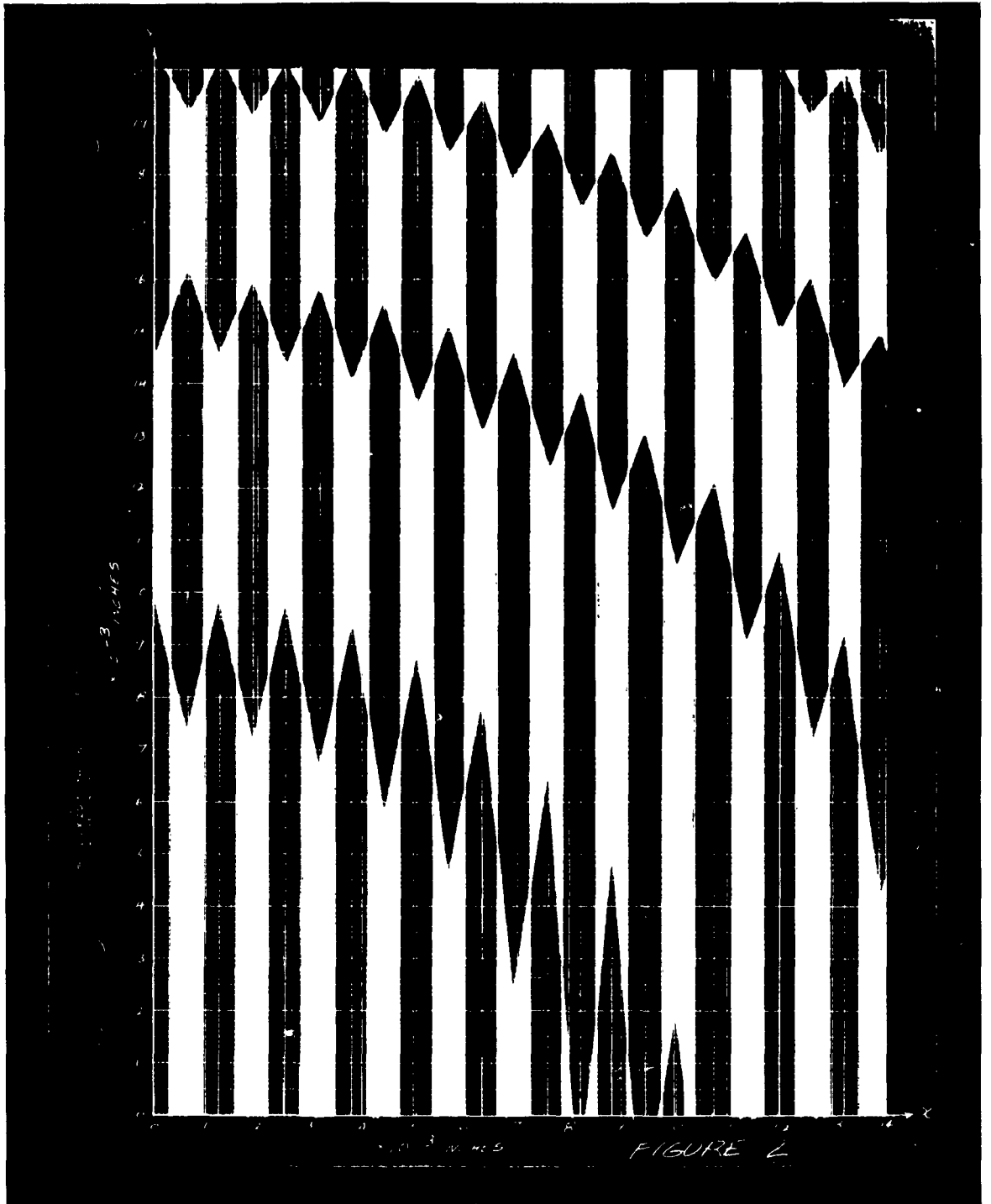


Figure C-2 - Hologram - Central Section

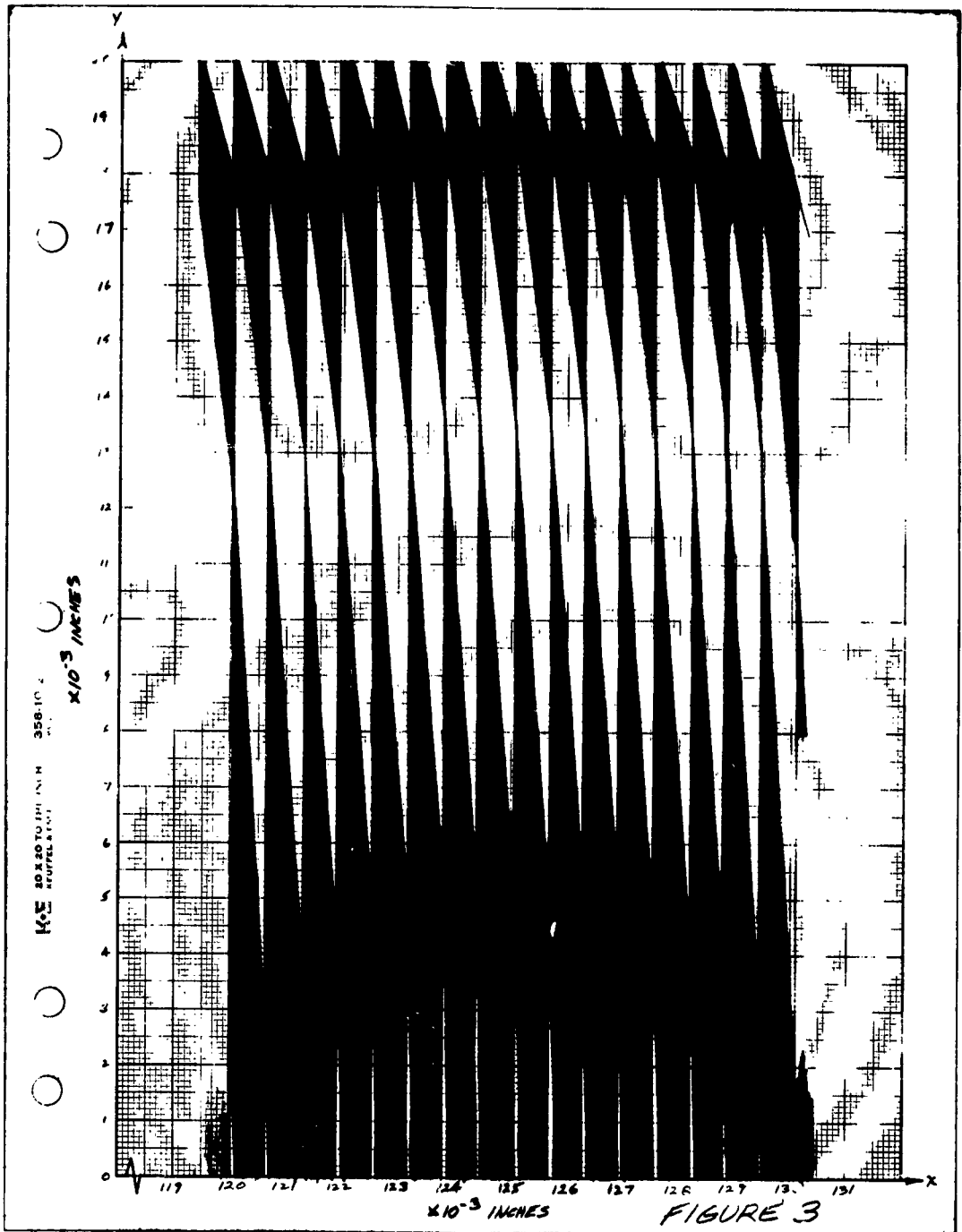


Figure C-3 - Hologram - Section Displaced From Center By Half
The Separation of Point Sources

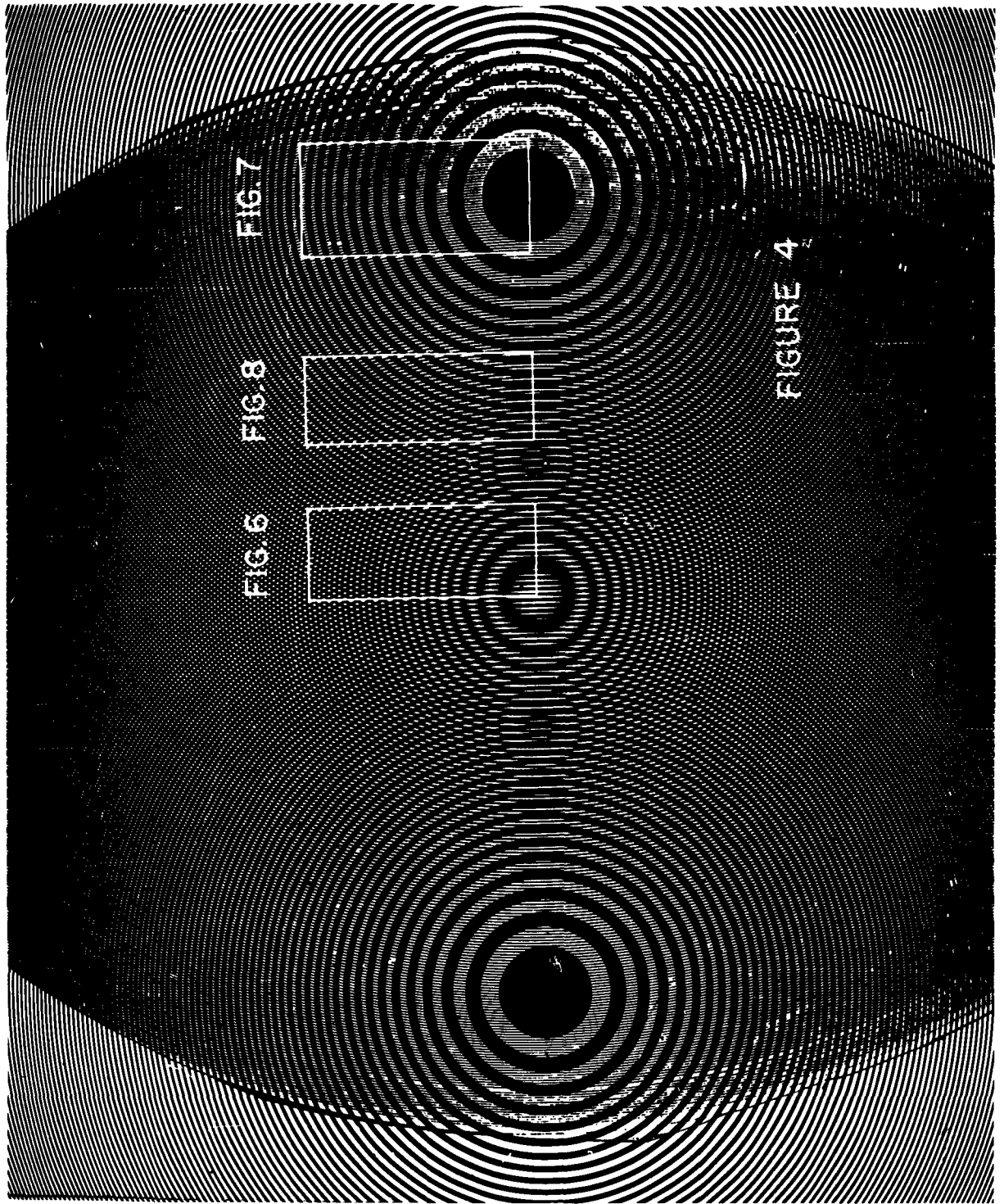


Figure C-4 - Overlapped Zone Plates
Zone Plate Centers Opaque

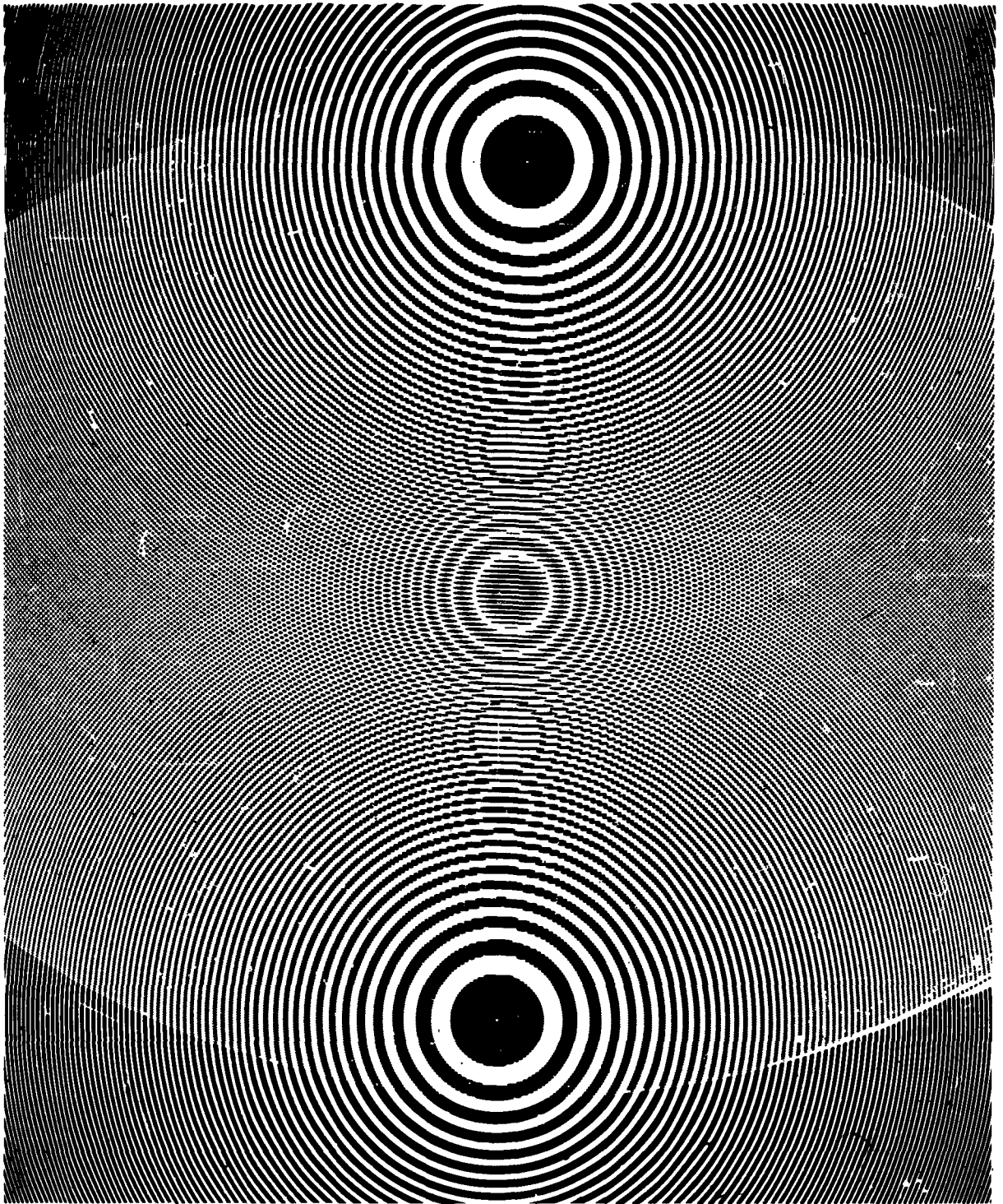


Figure C-5 - Overlapped Zone Plates
Zone Plate Centers Clear

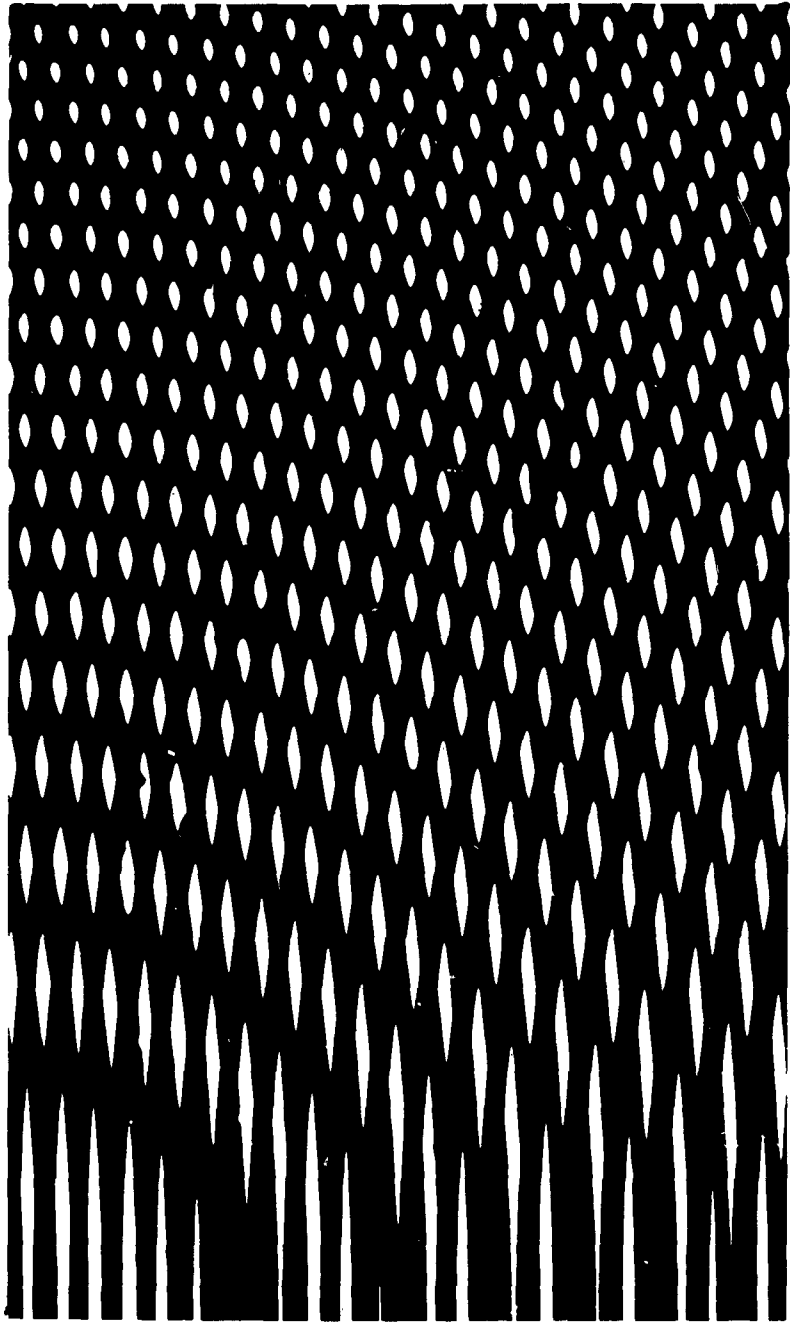


Figure C-6 - Overlapped Zone Plates - Enlarged Central Section

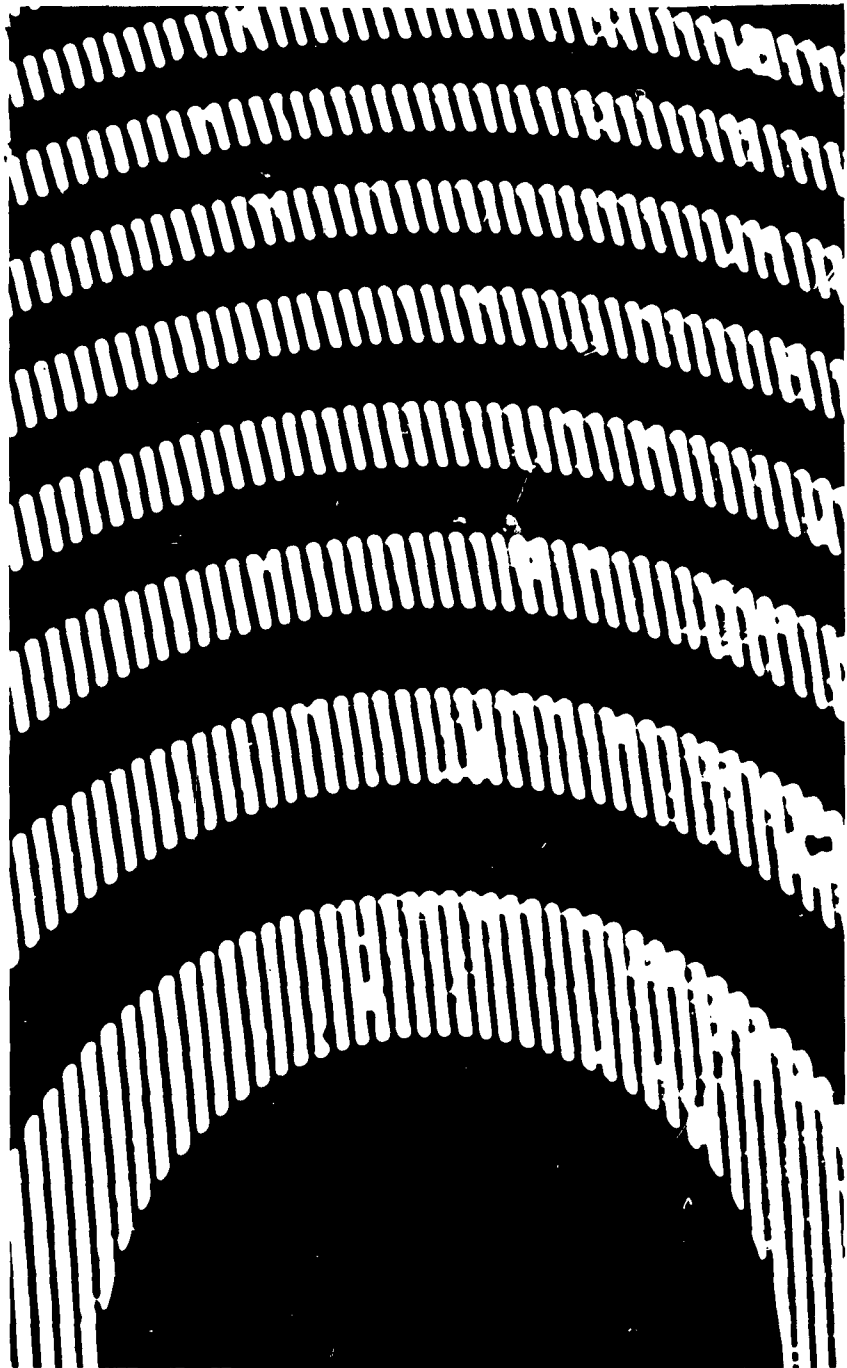
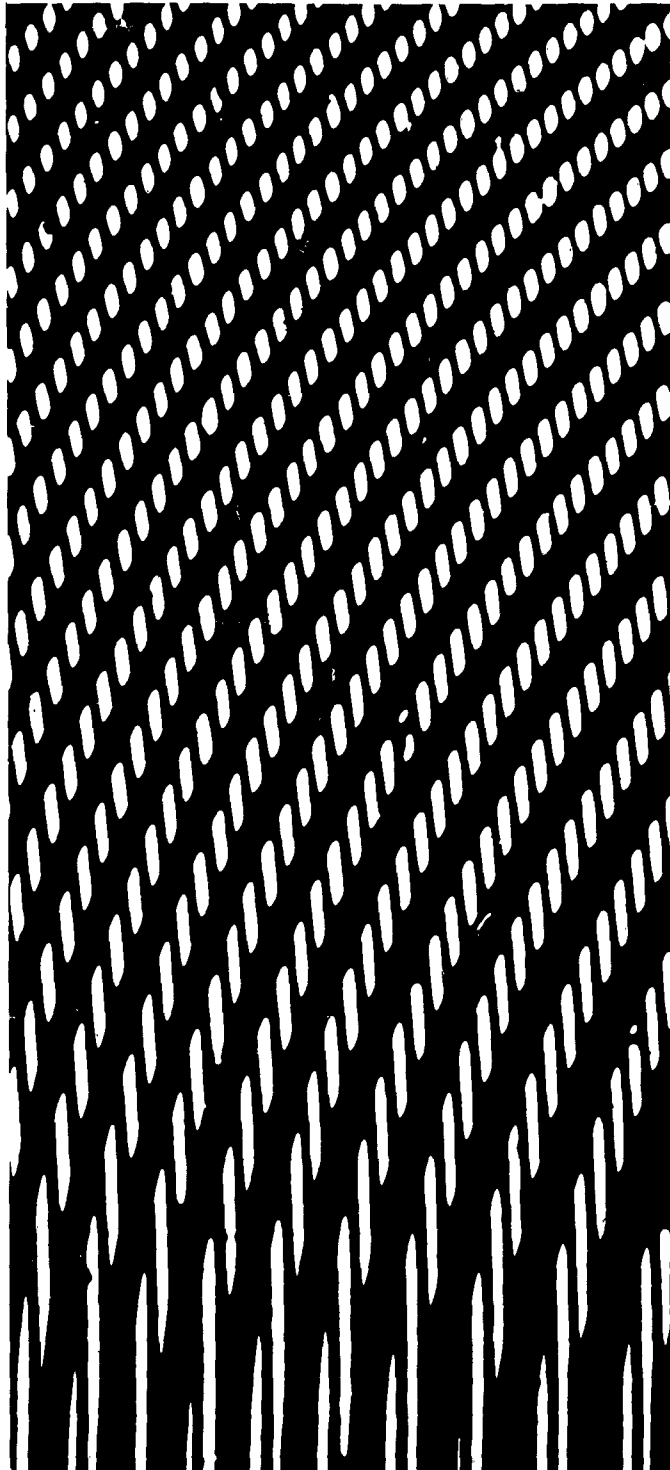


Figure C-7 - Overlapped Zone Plates - Enlarged Section
Around One Zone Plate Center



**Figure C-8 - Overlapped Zone Plates - Enlarged Section Between
Center of One Zone Plate And Center of Overlap Region**

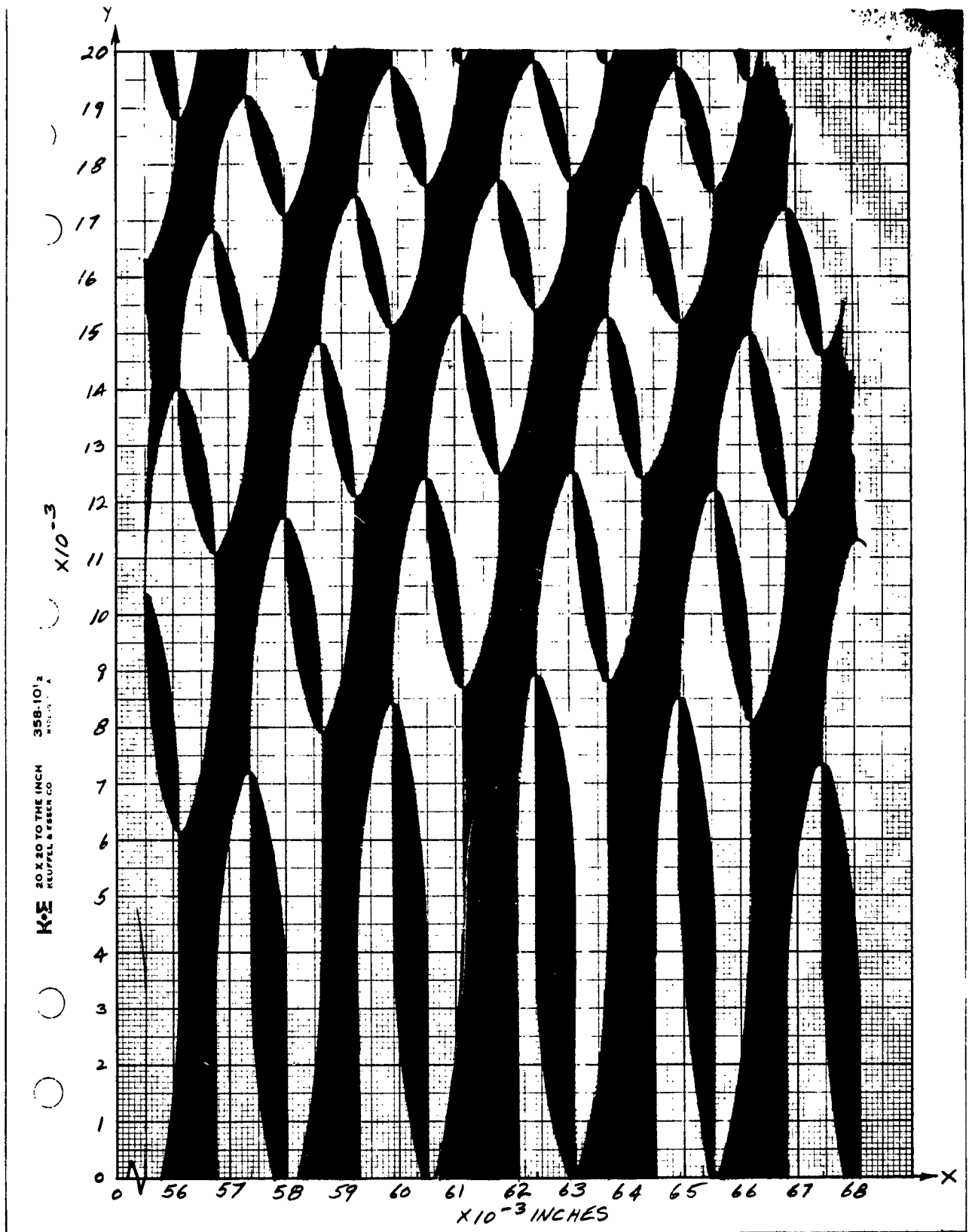


Figure C-9 - Hologram - Section Equivalent To Overlapped
Zone Plate (Fig. C-8)

C-14

The comparison of Figure C-6 with Figure C-2 and Figure C-7 with Figure C-3 illustrates the similarities and equivalencies of the patterns. In fact, the differences are in the fine detail only. Note particularly that the results of the calculation, as illustrated by Figure C-2, indicate that the interference pattern of two point sources and a plane wave produces an auxiliary zone plate centered at $x = y = 0$. This is in direct confirmation of our experience with overlapped zone plates.

Note also that in Figure C-4, another secondary zone plate (enlarged in Figure C-8) is produced mid-way between $x = 0$ and $x = \frac{d}{2}$ by overlapped zone plate pairs. The calculations were, therefore, extended to include this region as well. However, the use of (C.12) for this portion of the calculations was discarded in favor of an approach which proved less tedious and offered additional insight to the problem, i.e., (C.5) was transformed by trigonometric manipulation to

$$I = 4A^2 \left[2 + 2 \cos \frac{\pi}{\lambda} (s_2 - s_1) \cos \frac{\pi}{\lambda} (s_2 + s_1) - \sin^2 \frac{\pi}{\lambda} (s_2 - s_1) \right] \quad (C.13)$$

After performing the proper substitutions in (C.13), the result is

$$I = 4A^2 \left[2 + 2 \cos \left(\frac{\pi}{\lambda a} x d \right) \cos \frac{\pi}{\lambda a} \left(x^2 + y^2 + \frac{d^2}{2} \right) - \sin^2 \left(\frac{\pi}{\lambda a} x d \right) \right] \quad (C.14)$$

which proved easier to handle. The results are plotted in Figure C-9, which should be compared to Figure C-8 to note the equivalency. Again the differences are in the fine detail only.

The second term within the brackets of (C.13), by means of an identity, may be transformed such that (C.13) becomes

$$I = 4A^2 \left[2 + \cos \frac{2\pi}{\lambda} s_2 + \cos \frac{2\pi}{\lambda} s_1 - \sin^2 \frac{\pi}{\lambda} (s_2 - s_1) \right] \quad (C.15)$$

Setting $\cos \frac{2\pi}{\lambda} s_2$ and $\cos \frac{2\pi}{\lambda} s_1$ in (C.15) equal to zero yields two families of circles with origins at $(-\frac{d}{2}, 0)$ and $(\frac{d}{2}, 0)$, respectively. The radii of the circles are proportional to the square root of the number of the circle, or

$$r_n \propto \sqrt{n} \quad (C.16)$$

This is the same relationship that applies for the radii of Fresnel zone plates. Hence, $\cos \frac{2\pi}{\lambda} s_2 = 0$ and $\cos \frac{2\pi}{\lambda} s_1 = 0$ are the equations for the two zone plates which are overlapped in Figures C-4 and C-5.

APPENDIX D

SIMULTANEOUS TRACKING OF STAR FIELD AND COOPERATIVE SPACE VEHICLE

The simultaneous tracking of a star field and a cooperative space vehicle by a single (multi-function) sensor is an attractive concept in terms of a rendezvous mission. The attractiveness is enhanced if a single detector can be used for the simultaneous detection of the tracking error signals. In the case of the cooperative space vehicle containing its own light source, the modulation of the light source in a characteristic manner would permit - conceptually, at least - the use of the GPL correlation technique for simultaneous tracking of the star field and the cooperative space vehicle with but one detector. Hence the experimental demonstration of the concept received priority during the reporting period.

As presently conceived, the reference for the star field and beacon tracking correlator would be the usual Fresnel zone plate reference transparency with one modification: an additional zone plate would be positioned at the center of the reference transparency to permit simultaneous sensing of the beacon. The zone plate for the beacon would be properly scaled so that the diffraction image of the monochromatic light beacon is formed in the same plane as the star field correlation spot.

It may be recalled that ultra violet radiation is predominant in the spectral content of star light, and that the radiation decreases rapidly for longer wavelengths. Hence, assuming that the star field zone plates are proportioned such that the image formed by the near ultra violet radiation is focussed on the face of the detector, it would be desirable to select the wavelength of the light beacon from the red end of the spectrum in order to provide a certain amount of natural frequency selectivity by the zone plates for the area detector.

As a result of the above thinking, home-made blue and red filters were used in the first experimental set-up for the simulated star field and the beacon, respectively. A reference transparency, with the star field zone plates and beacon zone plate properly proportioned to take advantage of the filtering action, was made and used with an old demonstrator model of the GPL correlator.

The reference transparency, properly mounted in the GPL correlator, was jittered in azimuth a few degrees at a 25 cps rate, and the light beacon, simulated by a spot of light projected onto the simulated star field, was mechanically chopped at a 75 cps rate. The error signals, derived by moving the RTT area detector in X and Y by means of lead screws, were synchronously detected and observed both on an oscilloscope and a meter.

The bench set-up used in the demonstration is crude and unwieldy. Based on the encouraging results to date, however, the set-up will be re-worked for better simulation of the problem as well as to facilitate operation. As one of the improvements, the presently used red and blue filters, which are nothing more than red ink on glass and blue paper, respectively, will be replaced by Kodak Wratten gelatin filters. The filters are on order and delivery is expected shortly. In addition, means will be provided for moving the "beacon" across the simulated star field. Work has already begun on a new reference transparency to replace the hastily made prototype.

APPENDIX E

BEACON POWER REQUIRED ABOARD COOPERATIVE SPACE VEHICLE

Consideration of the feasibility of simultaneous tracking of a star field and modulated light beacon raises the question of the luminous power requirement for the beacon. Assuming that the luminous irradiance equivalent to a zero magnitude star will be sufficient for beacon tracking purposes, the problem to be considered may be defined as follows:

- a) Estimate the luminous power which must be transmitted by a beacon mounted on a space vehicle so that a second vehicle at a range of 1000 nautical miles will be irradiated by luminous power equivalent to the luminous irradiance from a zero magnitude star.
- b) Estimate the size, weight, and electrical power consumption of the equipment required to produce the luminous power established in (a) above.

The illumination produced by a $0^m.0$ star outside the earth's atmosphere is equal to 2.43×10^{-10} lumen/cm². One lumen at the wavelength of maximum visibility (0.556 μ) is equivalent to 1.47×10^{-3} watt. Therefore, the power density P of the irradiation in the visible region of the spectrum due to a $0^m.0$ star may be approximated by

$$P = 2.43 \times 10^{-10} \frac{\text{lumen}}{\text{cm}^2} \cdot 1.47 \times 10^{-3} \frac{\text{watt}}{\text{lumen}} \quad (\text{E.1a})$$

$$= 3.57 \times 10^{-13} \frac{\text{watt}}{\text{cm}^2} \quad (\text{E.1b})$$

To facilitate acquisition of the beacon signal for any orientation of the two vehicles, an isotropically radiating source as a beacon would be desirable if the power to be provided by the beacon does not thereby become excessive. The necessary luminous power that must be

radiated by the beacon (P_t) in order to provide the required power density (P) at a range (R) of 1000 nautical miles may be calculated as follows for an isotropically radiating source:

$$P_t = 4\pi R^2 P \quad (E.2a)$$

$$= 4\pi (1000 \text{ n.m.}) \left(\frac{1852 \text{ meters}}{\text{n.m.}}\right) \left(\frac{100 \text{ cm}}{\text{meter}}\right)^2 P \quad (E.2b)$$

$$= 1.54 \times 10^5 \text{ watts} \quad (E.2c)$$

Assuming a 50% transmitting duty ratio (square wave modulation) for the beacon, the average radiated beacon power (\bar{P}_t) is one-half P_t , or 7.7×10^4 watts for the isotropic source. This is evidently wasteful in terms of power. A value for \bar{P}_t 40 or 50 db down would be more acceptable. We will assume, therefore, the use of a reflector in the form of a section of a parabolic cylinder, utilizing a line source (as opposed to a point source), which will shape the radiated power into a fan beam that is wide in one dimension and narrow in the other.

Normally in antenna design, the amplitude and phase distribution over the aperture as well as reflector shape and size are strictly controlled to yield the desired beam pattern. A light source, such as might be used as the line source for the beacon, may be considered as an infinite number of point sources of random phase separated by infinitesimal distances. The line source may then be positioned coincident with the locus of the foci of the infinite number of parabolas (each separated by an infinitesimal distance) in the cylindrical parabolic reflector. Each point source is thus associated with a parabolic reflector of infinitesimal width and the result is a high directivity in one dimension.

To facilitate acquisition of the signal for any orientation of the two vehicles, the radiated power pattern in the transverse

dimension should approximate the rectangular power pattern of an isotropic source for 180 degrees. The reflector and line source (antenna) can then be rotated through 360 degrees at a constant angular rate in the plane perpendicular to the wide dimension, thus providing complete spherical coverage. As viewed from the receiving vehicle, the signal would be effectively modulated at a constant frequency.

The rectangular power pattern in the transverse dimension is a result of two factors: the randomness of the phases of the point sources comprising the line source does not permit directivity, while the reflector limits the transmission to the forward direction (180 degrees of arc if spill-over is neglected). The power pattern in the transverse dimension is, therefore, approximately a constant* for the beamwidth of 180 degrees.

Let us assume that we wish to limit the radiated luminous power of the beacon to 1.5 watts while still providing a power density equivalent to the irradiation in the visible region due to a 0^m.0 star to a vehicle at a range of 1000 n.m. Hence, the beacon must exhibit a directivity (D) of approximately 1×10^5 or 50 db, where directivity is defined as the ratio of maximum radiation intensity (U_m) from the source under consideration either to the radiation intensity (U_o) from an isotropic source, radiating the same power, or to the average radiation intensity (U_o) from the source under consideration.

If we now define the beam area (B) as the solid angle through which all the power radiated would stream if the power per unit solid angle equalled the maximum value U_m over the beam area,

$$U_m B = 4\pi U_o \quad (E.3)$$

and

$$\frac{U_m}{U_o} = D = \frac{4\pi}{B} \quad (E.4)$$

*The directivity would be approximately 2.

Defining θ and ϕ as the half power beamwidths in radians, the beam area is approximately equal to the product of θ and ϕ and we may say

$$D = \frac{4\pi}{\theta\phi} \quad (\text{E.5})$$

$$D = \frac{4.1253 \times 10^4}{\theta_1 \phi_1} \quad (\text{E.6})$$

where θ_1 and ϕ_1 are the half power beamwidths in degrees.

Since we have assumed that the beam pattern in the broad direction approximates that for an isotropic source for 180 degrees (and is non-existent for the other 180 degrees of the circle), we may set ϕ_1 equal to 180 degrees in (E.6) and solve for θ_1 , the half-power beamwidth in the transverse dimension.

Based upon a directivity of 1×10^5 (the radiated luminous power of the beacon is limited to approximately 1.5 watts), θ_1 is calculated as approximately 2.3×10^{-3} degrees or 8.3 seconds of arc.

For the purpose of comparison, we may assume that 15 watts of radiated luminous power is permissible, thus requiring a directivity of 1×10^4 . For ϕ_1 again set equal to 180 degrees, θ_1 then calculates to be 2.3×10^{-2} degrees or 83 seconds of arc.

The length (L_θ) of the aperture of the parabola (of the infinitesimal width) which determines the beamwidth in the θ direction may be calculated from

$$\theta_1 = \frac{58\lambda}{L_\theta} \quad (\text{E.7})$$

for a uniformly illuminated parabola, or from

$$\theta_1 = \frac{70\lambda}{L_\theta} \quad (\text{E.8})$$

if a 10 db taper is assumed.

Assuming the latter (pessimistic case), L_{θ} is calculated to be 3.04×10^4 wavelengths or 0.67 inch for the 1.5 watt case and 3.04×10^3 wavelengths or 0.067 inch for the 15 watt case. Of course, the figure of the parabola must be maintained with corresponding exactness.

The results of the above calculations are summarized in Table I to facilitate comparison.

TABLE I

D_1 , ϕ , θ and L_{θ} as a function of P_t for a
Line Source with a Cylindrical Parabolic Reflector

P_t (watts)	D	ϕ (degrees)	θ (degrees)	L_{θ} (λ)	L_{θ} (inches)
1.5	1×10^5	180	2.3×10^{-3}	3.04×10^4	0.67
15	1×10^4	180	2.3×10^{-2}	3.04×10^3	0.067

Two losses should be considered in determining the electrical power consumption of the beacon. The first concerns the efficiency of the line source. The American Institute of Physics Handbook* lists the absolute efficiencies (equivalent power in light flux per watt input) for various illuminants. The most efficient is the green fluorescent lamp with an absolute efficiency of 0.1235 watt of equivalent light flux per watt input. We will assume that a similar efficiency can be achieved with a line source.

The second loss which should be considered concerns the quality of the reflecting surface. Assuming that the reflecting surface of

*Pg. 6-77

the cylindrical parabolic reflector is silver plated in order to take advantage of its high reflecting property, a reflection efficiency of 0.85 may be assigned.

On the basis of the two losses discussed in the preceding paragraphs, the electrical power consumption of the beacon will be approximately 10 times the luminous power that the beacon must radiate, i.e., 15 watts for $P_t = 1.5$ watts and 150 watts for $P_t = 15$ watts. It becomes obvious that the latter figure is not as desirable as the former which is more in keeping with power consumption requirements acceptable for a space vehicle.

Assuming that the focus of the parabolic curvature of the reflector is in the plane of the aperture, and the line source at the focus employs a section of a cylindrical reflector to direct all radiation towards the cylindrical parabolic reflector, the size of the beacon should not exceed 1" x 3" x 1" if a suitable line source can be found or developed. Figure E-1 is a cross sectional sketch of the antenna. Its weight, including a drive motor and gearing, would probably not exceed 1/2 pound.

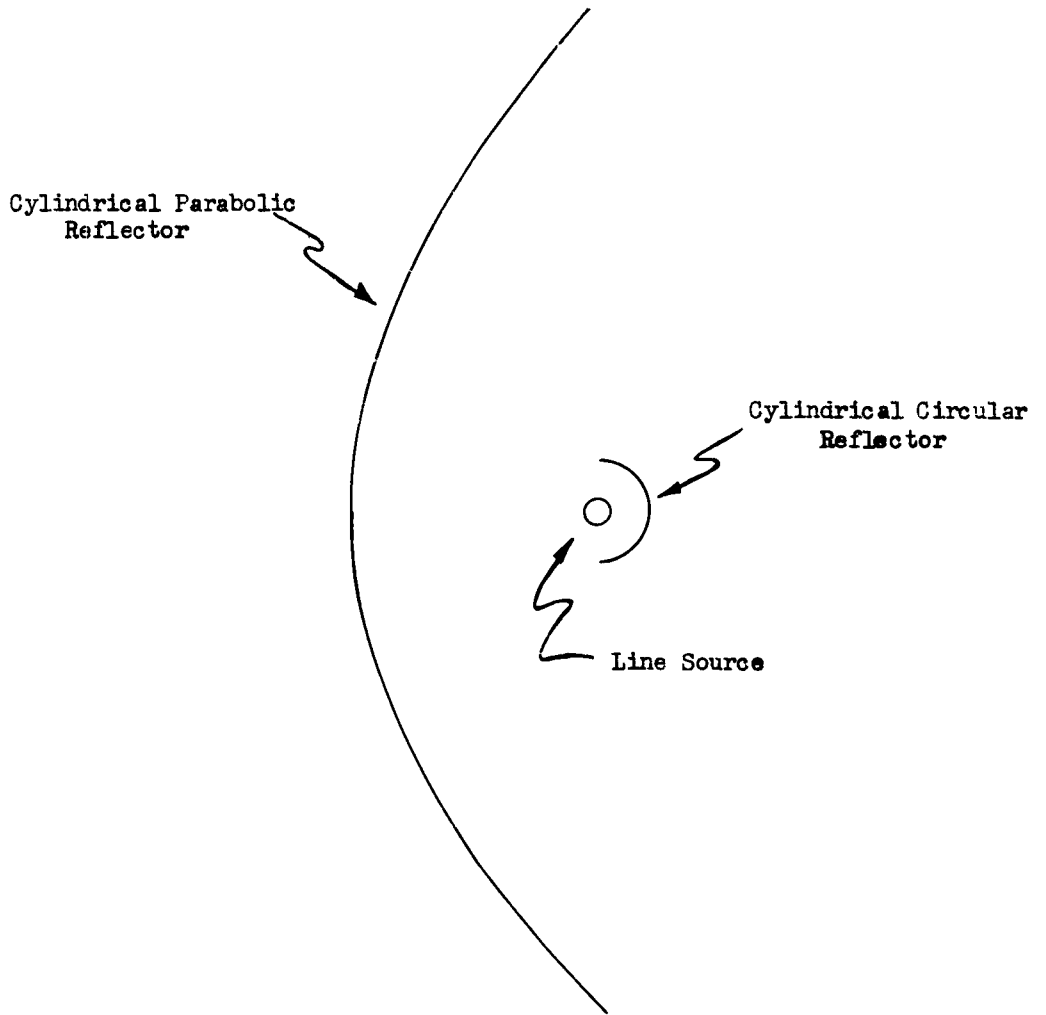


FIGURE E-1 - CROSS SECTIONAL SKETCH OF BEACON